Dalton Transactions

Accepted Manuscript

ROYAL SOCIETY OF CHEMISTRY

www.rsc.org/dalton

Dalton Transactions

ARTICLE TYPE

Safe disposal of radioactive iodide ions from solutions by Ag_2O grafted sodium niobate nanofibers

Wanjun Mu, Xingliang Li, Guoping Liu, Qianhong Yu, Xiang Xie, Hongyuan Wei, Yuan Jian*

Radioactive iodine isotopes are released into the enviroments by the nuclear industry and medical research institutions using the radioactive materials, which have negative effects on lives living within the ecosystem. Thus, safe disposal of radioactive iodine is necessary and emergency. For this reason, the uptake of iodide ions was investigated on Ag_2O nanocrystals grafted sodium niobate nanofibers, which were prepared by forming a well-matched phase coherent interface between them. The resulting composite was applied as an efficient adsorbent for I^- anions by forming an AgI precipitate, which also remained firmly attached to the substrates. Due to their one-dimensional morphology, the new adsorbents can be easily dispersed in liquids and readily separated after purification. This significantly enhances the adsorption efficiency and reduces the separation costs. The change in structure from the pristine sodium niobate to Ag_2O anchored sodium niobate and to the used adsorbent was examined by various characterization techniques. The effects of Ag^+ concentration, pH, equilibration time, ionic strength and competing ions on the iodide ions removal ability of the composite were studied. The Ag_2O nanocrystals grafted sodium niobate adsorbent showed high adsorption capacity and excellent selectivity for I^- anions in basic solutions. Our results are useful for the further development of improved adsorbents for removing of I^- anions from basic wastewater.

1 Introduction

After the nuclear accidents in Chernobyl (1986) and, more recently, Fukushima (2011), the concern on radioactive waste leakage rises to a higher level across the world.[1] The I^{131} isotope is a major product of uranium and plutonium

fission, making up nearly 3 wt % of the total fission products, and is also an important radioactive waste material from medical institutions owing to widely use in diagnosing and treating thyroid cancer.[2-3] Its potential toxicity arises from bioaccumulation through the food chain and subsequent dysfunction of the thyroid gland.[4-5] To address this serious issue, an efficient technology that can prevent the spread of radioactive iodine to the environment and allow its subsequent safe disposal must be developed. The key issue in the development of such a technology is to devise materials that are able to absorb radioactive iodine irreversibly, selectively, efficiently, and in large quantities from contaminated water. Various inorganic compounds, containing Bi(III),[6] Pb(II),[7] Hg(II),[8] Ag(I)[9] and Cu(II),[10] have been reported as adsorbents to form precipitates or sparingly soluble phases with I^- anions. The precipitates or sparingly soluble phases formed on the surface of a compound were then separated from the solutions and disposed safely. However, these compounds displayed low adsorption capacities and slow uptake dynamics due to their small specific surface areas. To solve this problem, Hg^{2+} cations were located onto the surface of natural zeolites to remove I^- anions from gaseous and aqueous wastes.[8] However, these zeolite adsorbents suffered from slow adsorption kinetics and thus, poor efficiency as most of the cations are located in the cages and channels of zeolite, which are less 1 nm wide. Diffusion of cations and anions through the narrow passages before their precipitation is slow. Such a drawback is intrinsic to the microporous structure of the substrates, impeding the practical application of zeolite based sorbents. Thus, the design and fabrication of new and highly efficient adsorbents in a low cost, simple and environmentally friendly manner is a significant challenge for environmental cleanup in real applications.

Ag_2O is a potential capture agent for the removal of I^- anions from water because it readily reacts with I^- anions to form insoluble silver iodide. However, the direct use of Ag_2O or another silver compound to precipitate iodine species is impractical as the adsorption capacity and dynamics of removal depend on the specific surface area of Ag_2O particles. When the specific surface area (large Ag_2O particles) is small, the removal ability of the material will be poor. Although the very fine Ag_2O particles with larger specific surface areas (small Ag_2O particles) may be used to improve the removal ability, the separation of the resulting AgI precipitates will be extremely difficult and expensive. A solution to this problem is to locate Ag_2O nanocrystals firmly onto a support with a large specific surface area that allow them to disperse sufficiently without forming the aggregates. For instance, novel nanomaterials based on Ag_2O grafted titanate and Ag_2O grafted layered sodium vanadate have been reported as adsorbents for highly efficient and selective capture of radioactive iodine.[11-12] In these cases, the Ag_2O nanocrystals were firmly bounded to the surface of the substrate materials through coherent interfaces. In addition, the morphology

of the substrate materials gave them a large surface area that provided space for the attachment of a large amount of Ag_2O nanocrystals and thereby increased the probability of contact with I^- anions,[12] and the AgI precipitates formed on the surface of the substrate materials were separated from solutions easily. These findings have highlighted a new direction for the synthesis of a grafted adsorbent for capturing radioactive iodine. Although Ag_2O nanocrystals anchored firmly and dispersed sufficiently onto the surface of supports with large specific surface areas, the application of such materials has until now been limited to neutral wastewater owing to the instability of the nanostructure supports in the practical basic media. Thus, the search of new supports that are stable under basic conditions is circular for the design of next - generation adsorbents.

Inorganic materials considered as the supports must possess some useful features, including a large specific surface area, the ability to firmly bind Ag_2O nanocrystals on the surface of the structure, and good resistance to radiation, heat, and chemicals. Sandia octahedral molecular sieves (SOMS) are a new family of octahedral microporous materials with niobate-based frameworks composed of $[NbO_6]$ and $[NaO_6]$ octahedral units, which endow these materials with abundant microporous structures, open tunnels and relatively high surface area.[13] Pure microporous phase SOMS $Nb_2Na_2O_6{\cdot}H_2O$ may be obtained from pentaethoxyl niobium solution through a hydrothermal method, which stably under wide range pH conditions and exhibited excellent resistance to radiation.[14] In addition, $Nb_2Na_2O_6{\cdot}H_2O$ nanomaterials having larger specific surface areas were obtained by optimizing the hydrothermal conditions. However, $Nb_2Na_2O_6{\cdot}H_2O$ is ineffective for the adsorption of radioactive anions such as iodine species, because it has both a permanently negatively charged surface like other aluminosilicate minerals and a pH-dependent negative surface charge caused by deprotonation of the surface hydroxyl group under high pH conditions.[15] Therefore, in this work, Ag_2O nanocrystals were anchored onto the surface of $Nb_2Na_2O_6{\cdot}H_2O$, and the resulting composite possessed a large specific surface area and high selectivity for the adsorption of radioactive iodine.

2 Experimental

2.1 Synthesis

All chemical used were purchased without further deal with unless otherwise specified. The 1D $Nb_2Na_2O_6{\cdot}H_2O$ nanofibers is prepared according to ref.13, in which 1g Nb_2O_5 and 60 mL of 10 mol L^{-1} NaOH solution were mixed under stirring at room temperature. The mixture was transferred into a 100 mL Teflon-lined autoclave and reacted at 180 °C for 2 h. After that, the autoclave cooled down naturally. The finally products were collected by glassware,

then washed with deionized water three times, and then dried in air at 80°C. For the synthesis of $Nb_2Na_2O_6 \cdot H_2O$ anchored with Ag_2O nanocrystals, 0.2 g $Nb_2Na_2O_6 \cdot H_2O$ were dispersed in 200 mL pure water. The pH value of the suspension was adjusted ~11 by dropwise addition of dilute NaOH solution. The nanoparticles were collected by centrifuging and then dispersed in 200 mL 0.01 − 0.03 mol L^{-1} silver nitrate aqueous solution. After stirring vigorously 24h, the precipitate was collected and washed with deionzed water three times, and then dried at 80 °C for 24 h. The composite obtained was named Ag_2O-$Nb_2Na_2O_6 \cdot H_2O$, according to the starting niobate. The processes of fabricating Ag_2O-$Nb_2Na_2O_6 \cdot H_2O$ compositions and I^- adsorption process are illustrated in Scheme 1.

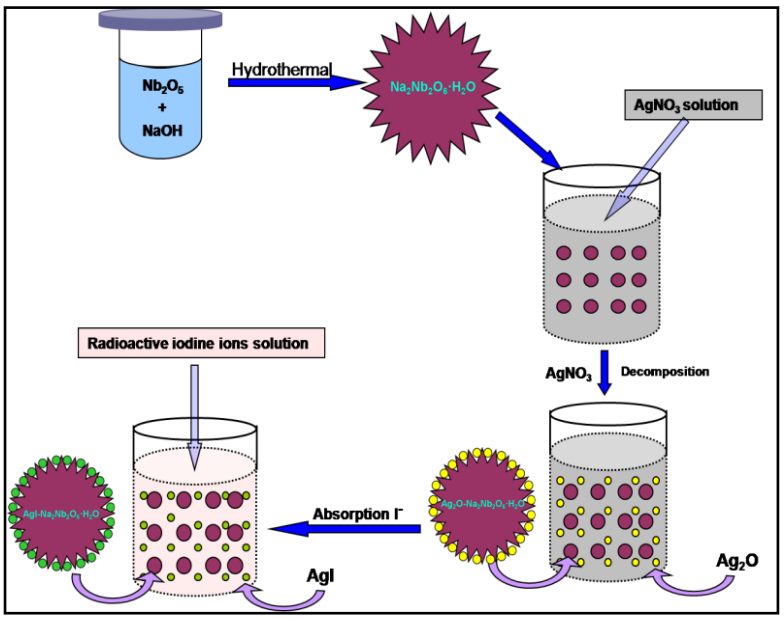

Scheme 1. Processes for fabricating Ag_2O-$Nb_2Na_2O_6 \cdot H_2O$ and AgI-$Nb_2Na_2O_6 \cdot H_2O$ composite

2.2 Adsorption capability

In this experiment, the anions adsorption experiments were carried out with nonradioactive in aqueous solution because of high radiation dose and toxicity of ^{131}I or ^{129}I. The equilibrium uptake capacities of the Ag_2O grated $Nb_2Na_2O_6 \cdot H_2O$ absorbents for I^- anions were conducted through batch experiments which were implemented using a series of concentrations of I^- solutions ranging from 50 ppm to 1000 ppm (the amount of adsorbent = 0.1g L^{-1}, 25°C, pH=9.0). For comparison, the same amount of $Nb_2Na_2O_6 \cdot H_2O$ was used as a control. The effects of Ag content and pH, equilibrium time, ionic strength and competition ions were examined. All the samples with iodide solutions were equilibrated for over 48 h at room temperature with magnetic stirring. Afterward the solids and solutions were separated by centrifugation and the supernatants were analyzed by ultraviolet spectrophotometer (UV−vis) to

determine the remaining iodide anions in the solutions. The sorption amount q_e (mmol g^{-1}) of adsorbed I^- ions is calculated as:

$$q_e = \frac{(C_0 - C_e) \times V}{m} \quad (1)$$

Where C_0 (mmol L^{-1}) is the initial concentration of metal ion, C_e (mmol L^{-1}) is the equilibrium concentration, V (L) is the volume of the testing solution and m (g) is sorbent dose.

2.3 Characterization

The crystalline structure of as-prepared samples were characterized using an X-ray diffraction (PXRD, X'Pert PRO, PANalytical, Almelo, Netherlands) with Cu-Ka radiation (λ=0.15406 nm at 40 kv and 45 mA). The sizes and shapes of the nanostructures were observed on a field emission scanning electron microscope (FE-SEM Philips XL30 FEG, Eindhoven, Netherlands) and transmission electron microscopy (TEM， JEM200CX, 120 kV). The composition and chemical state of X-Ray photoelectron spectroscopy (XPS) was performed on a RBD upgraded PHI-5000C ESCA system (Perkin-Elmer) using Mg-monochromatic X-ray at a power of 25 W with an X-ray-beam diameter of 10 mm, and a pass energy of 29.35 eV. The binding energy was calibrated by the C1s hydrocarbon peak at 284.8 eV. Nitrogen adsorption and desorption isotherms were measured at 77 K with a Beckman Coulter SA 3100 surface area analyzer. To determine the surface area, the Brunauer–Emmett–Teller (BET) method was used. Raman spectra were recorded on a microscopic confocal Raman spectrometer (Renishaw 1000 NR) with an excitation of 514.5 nm laser light.

2.4 Desorption Test of the Precipitated

Leaching or desorption was examined in various aqueous solutions. The 20 mg of adsorbents saturated with I^- anions were collected via the centrifugation and rinsed with deionized water three times to remove the remaining I^- anions in the solution and the adsorbents were dispersed into 20 mL of water or NaCl solutions. The suspension was stirred for different time at room temperature and the I^- anion concentrations of the solutions were determined by UV−vis spectroscopy as described above.

3. Results and discussion

3.1 Adsorption isotherms of iodine ions

The I^- anion equilibrium uptake isotherm of Ag_2O-$Na_2Nb_2O_6{\cdot}H_2O$ is shown in Fig.1a. This isotherm suggests that the maximum adsorption capacity of the Ag_2O-$Na_2Nb_2O_6{\cdot}H_2O$ for I^- anions was to be 2.33 m mol L^{-1} while that of the parent $Na_2Nb_2O_6{\cdot}H_2O$ was negligible. The uptake capacity of the Ag_2O-$Na_2Nb_2O_6{\cdot}H_2O$ compound is much higher than that of vanadate with anchored Ag_2O.[12] As shown in Fig.1b, the Ag_2O-$Na_2Nb_2O_6{\cdot}H_2O$ adsorbent was able to remove 80% of I^- anions from solution at initial I^- concentration as high as 200 ppm. More than 99% of I^- anions were removed when the initial concentration was 150 ppm or below. In stark contrast, the reaction of I^- anions with the parent (without Ag_2O nanoparticles) $Na_2Nb_2O_6{\cdot}H_2O$ was less than 1%, compared with that of Ag_2O-$Na_2Nb_2O_6{\cdot}H_2O$ shown above. Fig.S1 further proves that the adsorption capacity of Ag_2O-$Na_2Nb_2O_6{\cdot}H_2O$ depends on the Ag: Na ratio. Thus, we can adjust the properties of adsorbents to meet the different needs of variously contaminated water. Besides, its capacity of adsorption increased with temperature (Fig.S2). In this work, an Ag_2O-$Na_2Nb_2O_6{\cdot}H_2O$ composite with Na: Ag =1:3 was considered to be the optimum adsorbent. As shown in the inset photo of Fig.1a, the color of the Ag_2O-$Na_2Nb_2O_6{\cdot}H_2O$ adsorbent changed and a new phase identifiable as AgI was formed during the I^- uptake process, explained by Eq. (2) and the EDX results shown in Fig.S3f. Furthermore, the Ag_2O-$Na_2Nb_2O_6{\cdot}H_2O$ composite had high stability under thermal treatment because the nanostructure of $Na_2Nb_2O_6{\cdot}H_2O$ can easily be converted to perovskite phase by low-temperature heat treatment (500 –600 °C).[15] This property is favorable to bind up the absorbed iodine and thereby prevent secondary pollution during the radioactive waste disposal process.

$$Ag_2O(s) + 2I^-(aq) + H_2O \rightarrow 2AgI(s) + 2OH^-(aq) \qquad (2)$$

The kinetics of I^- uptake by Ag_2O-$Na_2Nb_2O_6{\cdot}H_2O$ adsorbent are plotted for different I^- anions concentrations of 0.5, 1.0, and 1.5 mmol L^{-1} as shown in Fig. 1c. The removal percentage for I^- anions reached 97, 92, and 89% on Ag_2O-$Na_2Nb_2O_6{\cdot}H_2O$ within the first 60 min at the initial concentration of 0.5, 1.0, and 1.5 mmol $L^{-1,}$ respectively, and the I^- anions could be captured completely in 110 min. Compared with the kinetics of traditional active carbon and other micomaterials,[17-18] the present Ag_2O-$Na_2Nb_2O_6{\cdot}H_2O$ adsorbent is faster and thus more efficient for the removal of I^- anions. This is because the adsorption mechanism is based on the preferable chemical reaction between I^- anions and Ag_2O rather than physical adsorption where adsorption is established by sufficient surface contact and distribution between adsorbate and adsorbent which usually takes considerable amount of time to reach adsorption equilibrium. In addition, the parent $Na_2Nb_2O_6{\cdot}H_2O$ composed of nanofibers with a larger special surface area possesses more space

for the attachment of Ag_2O particles, which provides more opportunities for I^- anions and adsorbents to come into contact. Therefore, the surface area of the substrate materials is a crucial parameter that determines the adsorption capacity and efficiency of adsorbent. The nanofibers morphology of Ag_2O-$Na_2Nb_2O_6{\cdot}H_2O$ adsorbent was founded to be maintained after uptake of I^- anions (Fig.S3), which ensures that the adsorbents settled in the solution within 60 min, enabling its facile separation from the solutions for ultimate safe disposal. The important property could greatly reduce the cost of separation and make it feasible for practical application.

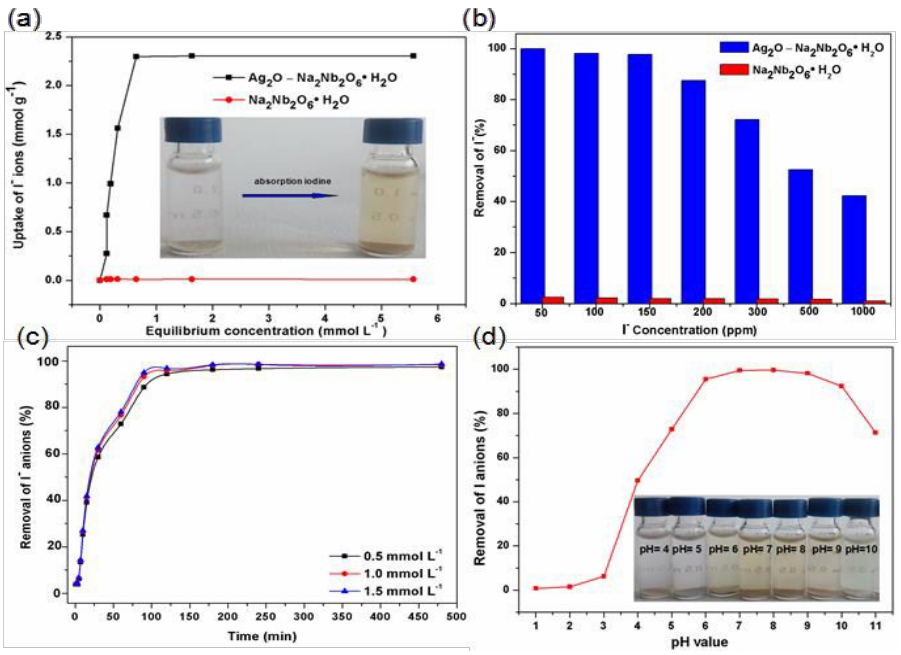

Fig.1. Removal of iodide anions from solutions by Ag_2O-$Na_2Nb_2O_6{\cdot}H_2O$. (a) I isotherms of uptake by Ag_2O-$Na_2Nb_2O_6{\cdot}H_2O$ and $Na_2Nb_2O_6{\cdot}H_2O$ over 48 h (25 ℃, pH = 9.0). The photo in the inset depicts the adsorbent in aqueous solution (left) and sedimentation changes after adsorption of I^- (right). Deionized water was used as a control. (b) I^- removals as a function of initial anion concentration in water. (c) I^- adsorption kinetics of Ag_2O-$Na_2Nb_2O_6{\cdot}H_2O$ for different initial concentrations. (d) Percentage removed I^- anions in the pH range of 1–11. Inset: color change of adsorbent in aqueous I^- solutions of different pH values.

The pH value of the medium was one of the factors that most affected the I^- adsorption behavior on the adsorbent by inducing a change in its surface charge, as shown in the Fig.1d. The uptake ability of Ag_2O-$Na_2Nb_2O_6{\cdot}H_2O$ for I^- anions is low in acidic media (pH < 6), because Ag_2O nanoparticles could partly dissolve and lose their ability to capture I^- anions. The maximum adsorption capacity was obtained in the pH range of 6 – 9. However, the uptake efficiency of the Ag_2O-$Na_2Nb_2O_6{\cdot}H_2O$ adsorbent had a slight decrease in basic conditions. For instance, an initial concentration of 100 ppm I^- was completely removed in near-neutral solution (pH = 6). However, only 50% of the same concentration of I^- anions was removed by the Ag_2O-$Na_2Nb_2O_6{\cdot}H_2O$ adsorbent when the pH was increased to

11. This is because the negative charges of the adsorbent surface increases with the increase of OH^- ions concentration at high pH, thus the uptake efficiency of adsorbent for I^- anion decreases. Therefore, the color of the adsorbent gradually became weaker in strong acid and basic environments (Inset of Fig.1d). Table 1 shows a comparison of the I^- anions adsorption capacities of various adsorbents. It is apparent that the present Ag_2O-$Na_2Nb_2O_6{\cdot}H_2O$ absorbent exhibited much higher adsorption capacity for I^- anions in basic conditions than previously studied Ag_2O-based adsorbent and thus has good potential for applications in practical radioactive wastewater treatment.

Table 1. Comparison of the maximum I^- adsorption capacities of Ag_2O-$Na_2Nb_2O_6{\cdot}H_2O$ and other Ag_2O-based adsorbents

Adsorbents	Experiment media	Adsorption capacity of I^- anions ($mmol\ g^{-1}$)	Reference
Ag_2O- Vanadate	water	1.7	11
Ag_2O-T3NL	water	3.4	19
Ag_2O-Ag/TiO_2	water	1.64	20
Ag_2O-T3NF	water	4.5	12
Ag_2O-T3NT	water	3.0	12
Ag_2O-$Na_2Nb_2O_6{\cdot}H_2O$	basic media (p H=9.0)	2.3	this work

3.2. **Structure and Morphology of Used Absorbent**

The parent $Na_2Nb_2O_6{\cdot}H_2O$ possesses a framework structure composed of layers of edge- sharing [NbO_6] octahedra, and the exposed plane is (200) (Fig.S4). XRD analysis revealed the structural evolution of the adsorbent from the pristine $Na_2Nb_2O_6{\cdot}H_2O$ to Ag_2O-$Na_2Nb_2O_6{\cdot}H_2O$ and the used adsorbent. Compared with $Na_2Nb_2O_6{\cdot}H_2O$, profound structural changes can be observed from the XRD pattern of Ag_2O-$Na_2Nb_2O_6{\cdot}H_2O$, although it is difficult to observe the diffraction peaks of Ag_2O nanocrystals from the XRD patterns. As shown in the Fig.2, the most obvious change was the disappearance of the (200) plane diffraction peak after precipitation of Ag_2O nanocrystals on the surface of the $Na_2Nb_2O_6{\cdot}H_2O$. When most of the Ag^+ ions form $Ag(OH)_n(H_2O)_m$ intermediates on the surface of

$Na_2Nb_2O_6{\cdot}H_2O$ in neutral or basic solution. These unstable intermediates will bond to the surface of the $Na_2Nb_2O_6{\cdot}H_2O$ by sharing the surface oxygen atoms of NbO_6 octahedron slabs in the (200) plane. The sharing of surface oxygen atoms cause serious deformation of the surface plane (200), leading to a loss in diffraction intensity of this plane. Meanwhile, the rest of the Ag^+ will move into the interlayer space, exchanging with Na^+ ions within the interlayer space, and have the strong interactions with the surrounding oxygen atoms. This causes the oxygen atoms to be slightly moved from their initial position, leading to a decrease in diffraction intensity and deterioration of crystallinity. After the capture of I^- anions, AgI nanocrystals will be formed on the surface of the $Na_2Nb_2O_6{\cdot}H_2O$ nanofibers. However, the serious deformation of the $Na_2Nb_2O_6{\cdot}H_2O$ nanostructure is still retained after the reaction with I^- anions because the phase interface between AgI nanocrystals and the $Na_2Nb_2O_6{\cdot}H_2O$ surface is composed of silver atoms and oxygen atoms of Nb-O frameworks (Fig. 2f). The corresponding change in structure of $Na_2Nb_2O_6{\cdot}H_2O$ can be further determined by Raman spectroscopy (Fig. S5). The intensity of the peak at 885cm^{-1} corresponding to the short Nb=O stretching mode decreased after contacting with Ag^+ ions, and its position shifted to low frequency. Meanwhile, the peak at 599 cm^{-1} which is assigned to the O-Nb-O stretching mode, exhibited a slight shift. The bands at 965 and 1120 cm^{-1} corresponding to the very short Nb-O bond in NbO_6 octahedra disappear after the deposition of Ag_2O nanocrystals. Furthermore, the XPS spectra of Ag_2O- $Na_2Nb_2O_6{\cdot}H_2O$ has confirmed the existence of Ag_2O nanocrystals although the diffraction peaks are absent in XRD patterns. As shown in the Fig.S6, a characteristic of Ag_2O crystals is located at 357.6 e V, which corresponds to Ag3d $_{2/5}$.

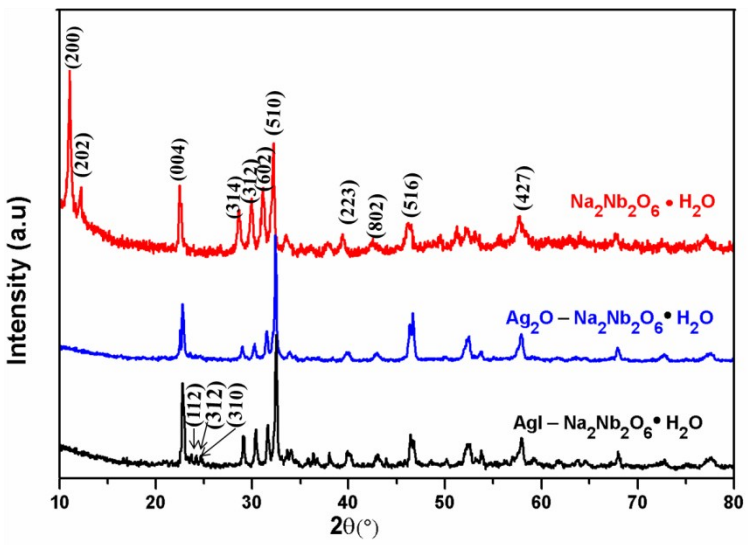

Fig.2. XRD patterns of the $Na_2Nb_2O_6{\cdot}H_2O$, Ag_2O-$Na_2Nb_2O_6{\cdot}H_2O$ and AgI -$Na_2Nb_2O_6{\cdot}H_2O$. Inset shows an enlargement of the selected area.

The morphological features of the as-prepared products were determined by scanning electron microscopy (SEM) (Fig.S3). The images clearly show that a nanofiber morphology with an average diameter of 200 – 300nm was maintained both after the deposition Ag_2O nanocrystals and the uptake of I^- anions. Considering the EDX results (Fig.S3e) of the total loading of Ag, the content of Ag^+ can be calculated, namely 24.85 mg. High-resolution transmission electron microscopy (HRTEM) investigations indicated that a larger of Ag_2O naoparticles with a size of 3 – 5 nm were well dispersed on the external surface of $Na_2Nb_2O_6{\cdot}H_2O$ nanofibers when they were deposited from an aqueous silver nitrate solution under neutral or basic condition (Fig. 2a, 2b). Although the nanaocrystals population is high, there is no crystals aggregation observed. This ensures the maximum exposure of all Ag_2O nanocrystals to the contaminated water and thus a high efficiency of capturing I^- anions. Furthermore, the amount of Ag_2O nanocrystal on the surface of the $Na_2Nb_2O_6{\cdot}H_2O$ nanofibers was readily controlled by adjusting the concentration of Ag^+ ions in the aqueous silver nitrate solution (Fig. S7).

To capture and immobilize I^- anions from wastewater, the key issue is that the Ag_2O nanoparticles must be firmly attached to the $Na_2Nb_2O_6{\cdot}H_2O$ nanostructures. If they readily detached from the substrates, it would be extremely difficult and expensive to recover the fine nanoparticles from solution. In addition, if not well dispersed on the $Na_2Nb_2O_6{\cdot}H_2O$ nanostructure, the small Ag_2O nanoparticles may aggregate together to form a solid with a low surface area and thus poor ability to precipitate I^- anions. Fortunately, the Ag_2O nanoparticles were located on the external surface of the $Na_2Nb_2O_6{\cdot}H_2O$ nanofibers because they had a similar surface crystal structure, as shown in the inverse fast Fourier transform (IFFT) image (Fig. 3c) of the selected area in Fig.3b. The interplanar distance of the (111) planes of the Ag_2O nanocrystals was 0.2748 nm, which was close to that of the (510) plane of the $Na_2Nb_2O_6{\cdot}H_2O$ nanofibers (0.2742 nm). If every (111) plane of Ag_2O matches with every (510) plane of the $Na_2Nb_2O_6{\cdot}H_2O$ nanofibers when the Ag_2O nanocrystals and $Na_2Nb_2O_6{\cdot}H_2O$ substrate join at these surfaces, the number of oxygen atoms shared by the two phases is maximized and full coordination can be achieved to form a well-matched interfaces (coherent interfaces). Such coherence between the two phases can reduce the overall energy by minimizing the surface energy and anchor the Ag_2O nanoparticles on the external surface of the 1-D $Na_2Nb_2O_6{\cdot}H_2O$ nanostructure. Fig.3d shows a HRTEM image of the used adsorbents. It can be seen that after adsorption of I^- anions, the formed AgI nanocrystals were slightly larger (5 – 8nm) than the initial Ag_2O nanoparticles anchored on the surface of the $Na_2Nb_2O_6{\cdot}H_2O$ nanofibers. The presence of iodine in the used absorbents was also confirmed by EDS (Fig.S4), XRD (Fig.2), and XPS (Fig.S6). The IFFT of the used adsorbent

(Fig.3f of the selected area in Fig.3e) showed that the interplanar distance of the $(11\bar{2}0)$ planes of the AgI nanocrystal was 0.2290 nm, close to that of the (111) planes of the $Na_2Nb_2O_6{\cdot}H_2O$ nanofibers (0.2250nm), the two phases were able to join to form a well-matched interface that bonded the newly deposited AgI nanocrystals firmly to the $Na_2Nb_2O_6{\cdot}H_2O$ nanofibers.

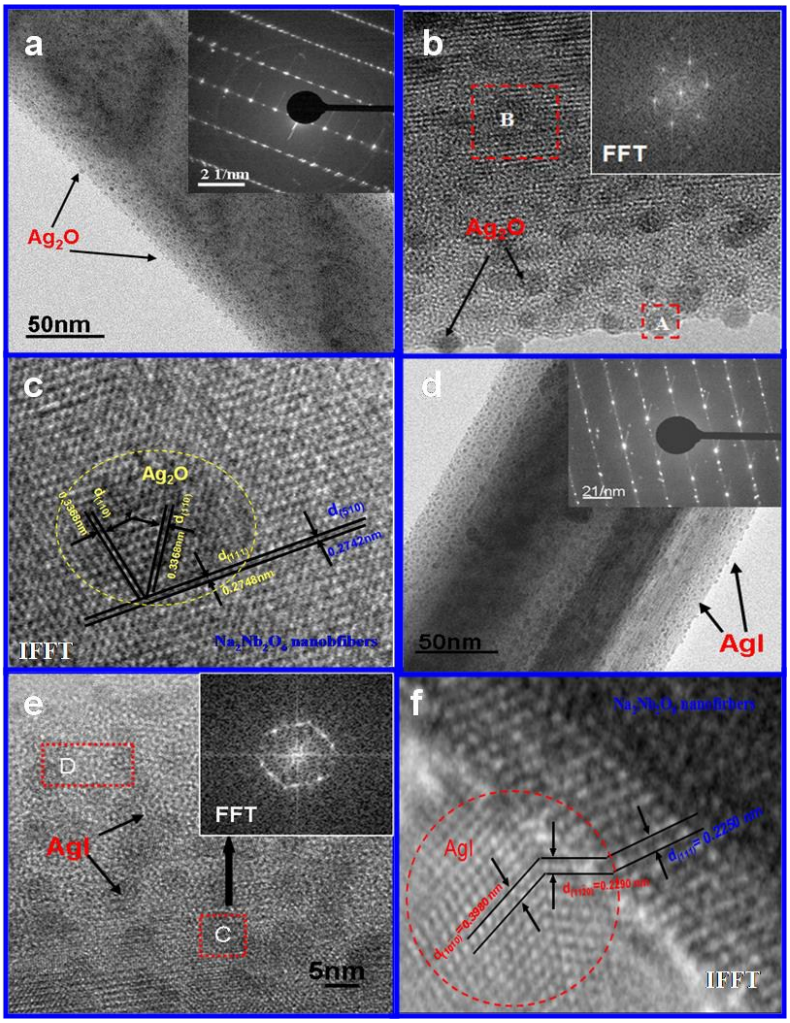

Fig. 3. TEM images of $Na_2Nb_2O_6{\cdot}H_2O$ nanofibers anchored with Ag_2O nanocrystals (Ag_2O-$Na_2Nb_2O_6{\cdot}H_2O$) and $Na_2Nb_2O_6{\cdot}H_2O$ nanofibers anchored with AgI nanocrystals (AgI-$Na_2Nb_2O_6{\cdot}H_2O$). (a) TEM image showing the abundant Ag_2O nanocrystals dispersed on the $Na_2Nb_2O_6{\cdot}H_2O$ nanofibers. Inset: SAED image of a signal nanofiber. (b) HRTEM image of Ag_2O nanoceystals. Inset: FFT image of the selected area A. (c) IFFT image of the selected area B in (b). (d) TEM image of AgI nanocrystal formed on a signal $Na_2Nb_2O_6{\cdot}H_2O$ nanofibers. Inset: SAED image of a signal nanofiber. (e) HRTEM image of AgI nanocrystals on $Na_2Nb_2O_6{\cdot}H_2O$. Inset: FFT image of the selected area C. (f) IFFT image of the selected area D in (e).

The BET surface area of $Na_2Nb_2O_6{\cdot}H_2O$ nanofibers (152 $m^2\ g^{-1}$) is calculated from the nitrogen isotherms in Fig.4, which shows typical type-II isotherms and H3 -type hysteresis loops. The surface area of the substrate material is a crucial parameter for adsorbent in terms of its adsorption capacity and efficiency. The $Na_2Nb_2O_6{\cdot}H_2O$ nanofibers

obtained in this work had a large amount of space available for the attachment of a large amount of Ag_2O nanocrystals, which provides more contact opportunities for I^- anions. In addition, the larger surface area and nanofibers structure allowed the fast adsorption of I^- anions from solution without diffusion problem. It was also found that the surface area of the $Na_2Nb_2O_6{\cdot}H_2O$ decreased after Ag_2O nanoparticles grafted on their surface.

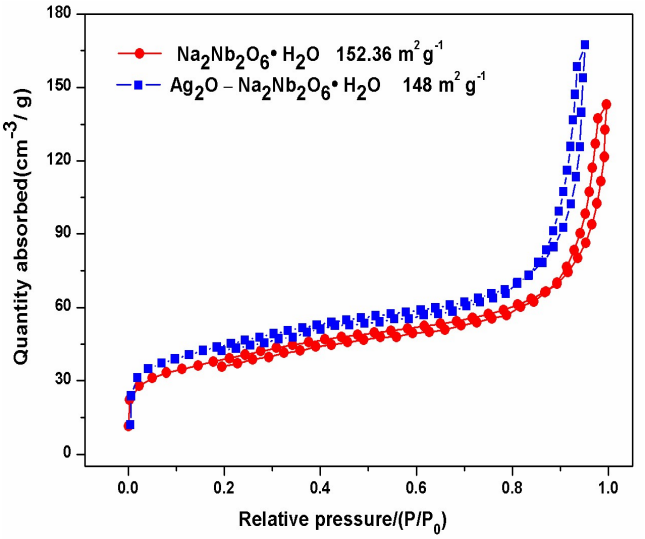

Fig.4. N_2 adsorption-desorption isotherms for Ag_2O-$Na_2Nb_2O_6{\cdot}H_2O$ and $Na_2Nb_2O_6{\cdot}H_2O$

3.3. Selective uptake and Leaching test

To investigate the selective uptake of I^- anions uptakes by the Ag_2O-$Na_2Nb_2O_6{\cdot}H_2O$ adsorbent, we conducted uptake tests in the presence of different concentrations of Cl^- anions. As shown in Fig. 5a, more than 98% of I^- anions were taken up by Ag_2O-$Na_2Nb_2O_6{\cdot}H_2O$ absorbent in 0.001 – 0.100 mol L^{-1} NaCl solutions. Clearly, the Ag_2O-$Na_2Nb_2O_6{\cdot}H_2O$ absorbents had high selectivity for I^- anions and competing Cl^- anions had little effect on its I^- ions uptake capacity. This result should be attributed to the large difference in the Gibbs energy of the reactions between Ag_2O and I^-, and Ag_2O and Cl^- anions.[12] The energy for the reactions between Ag_2O and I^- (-32 kJ mol^{-1}) is lower than that for the reaction between Ag_2O and Cl^- (+41 kJ mol^{-1}).[11] Thus, AgI precipitates formed more easily than AgCl precipitates under the same conditions.

Leaching tests of the used adsorbents were conducted to evaluate the adsorption reversibility of the Ag_2O-$Na_2Nb_2O_6{\cdot}H_2O$ adsorbent. Adsorption irreversibility is desirable for radioactive waste treatment because it can ensure that adsorbed radioactive species are not released and thus prevent secondary pollution. The leaching experiment was carried out in pure water for several days (Fig. 5b). It was found that the quantity of I^- anions released from the used

adsorbent was very low or below detection limits, and was almost unchanged with increasing temperature (Fig. S8). In addition, the presence of Cl^- anions in the water had little effect on the concentration I^- anions leached. Evidently, owing to its superior adsorption properties, the present Ag_2O-coated $Na_2Nb_2O_6 \cdot H_2O$ adsorbent is a potential candidate for practical application in wastewater treatment.

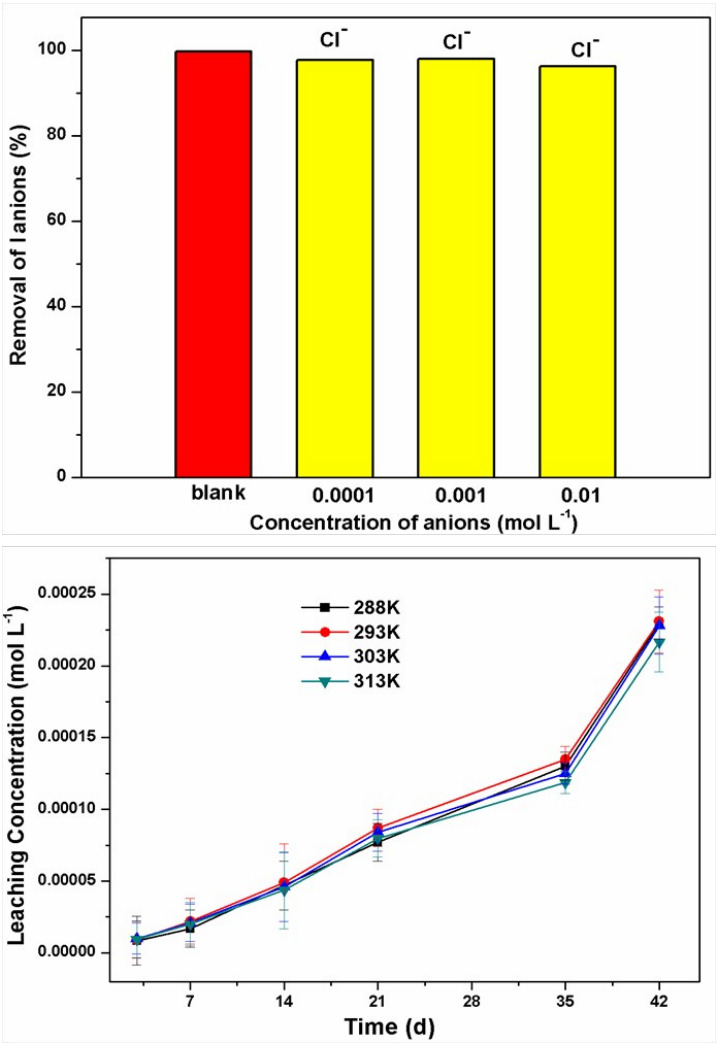

Fig.5. (a) Effect of Cl^- concentration on the removal of I^- anions by Ag_2O–$Na_2Nb_2O_6 \cdot H_2O$ (b) Effect of temperature on the leaching of I^- anions from used adsorbent in water.

Conclusions

This study demonstrates that the unique structural features, good basic resistance, and high selectivity of the Ag_2O-$Na_2Nb_2O_6 \cdot H_2O$ make it superior, effective and irreversible adsorbent for the removal of radioactive iodine from basic wastewater. The nanofiber structure of this material provides a larger surface area, which not only assures a high capacity for the uptake of iodide ions and very fast kinetics, but also allows a facile recovery of the adsorbent from

the ultimate solutions for safe disposal. The Ag_2O-$Na_2Nb_2O_6 \cdot H_2O$ nanofibers as a adsorbent exhibited performance in basic media much better than that of Na titanate nanostructures (T3NT, T3NF and T3NT). This study further indicates that the Ag_2O-based adsorbent with the nanostructure are potential candidates for new 'intelligent' adsorbents used for removal of other toxic anions from various wastewater.

Acknowledgments

We wish to acknowledge the financial support from the Foundation of China Academy of Engineering Physics and the National Natural Science Foundation of China (no: 21501159)

Notes and references

1. M. Asami and M. Akiba, *Journal of National Institute of Public Health.*2011,.60,306-313.
2. H. A. Robertson and I. R. Falconer, *Nature*. 1959, 184, 1699-1702.
3. T .H. Woo, *Ann. Nucl. Energy*. 2013, 53, 197–201.
4. J. A. Franklyn, P. Maisonneuve, M. C. Sheppard, J. Betteridge and P. Boyle, *N. Engl. J. Med.* 1998, 338, 712-718.
5. P. Vitti, F. Delange, A. Pinchera, M. Zimmerman and J. T. Dunn, *Lancet.*2003, 361, 1226-1231.
6. P. Taylor and V. Lopata, *J. Can. J. Chem*. 1988, 66, 2664-2670.
7. H. Kodama, *Czech. J. Phys*. 1999, 49, 971-977.
8. S. D.Balsley, P. V. Brady, J. L. Krumhansl and H. L. Anderson, *Environ. Sci. Technol*. 1996, 30, 3025-3027.
9. B. Grambow, *J. Contam. Hydrol*. 2008, 102, 180-186.
10. G. Lefevre, A. Walcarius, J. J. Ehrhardt and J. Bessiere, *Langmuir*. 2000, 16, 4519-4527.
11. S. Sarin, B. Arixin, L. Dejun, H. W. Liu, D. J. Yang, C. F. Zhou, N. Maes, S. Komarneni and H.Y. Zhu, *Chem. Mater*. 2014,26,4788-4795.
12. D. J. Yang, S. Sarina, H. Y. Zhu, H. W. Liu, Z. Z. Zheng, M. X. Xie, S. Smith and S. Komarneni, *Angew. Chem. Int. Ed.* 2011, 50, 10594-98.
13. M. Nyman, A. Tripathi, J. B. Parise, R. S. Maxwell, T. M. Nenoff, *J. Am. Chem. Soc.* 2002,124, 1704-1710.
14. H. Y. Zhu, Z.F. Zheng, X.P. Gao, Y. N.Huang, Z .M. Yan,Jin Zou, H. M. Yin, Q. D. Zou, K.Scott H, J.C. Zhao, Yunfei Xi, W. N. Martens and R. L. Frost, *J. Am. Chem. Soc.*2006, 128, 2373-2384.

15. M. Nyman, A. Tripathi, J.B. Parise, R. S. Maxwell, W. T. A. Harrison, T. M. Nenoff, *J. Am. Chem. Soc*. 2001, 123, 1529-1533..

16. C. Sungwook, K. Minkyung, Y. Jungseok, K. Mingyu, U. Wooyong, *Environ. Sci. Technol*. 2014, 48, 9684-9691.

17. J. B. Zhou, S. Hao, L.P. Gao and Y. C. Zhang, Annals of Nuclear Energy, 2014,72,237-241.

18. I. Marya, M. Yoshihiko, S. Yute, M. Taku and S. Nobutaka, Water. Res, 2015, 68, 227-237.

19. A. Bo, S. Sarina, Z. F. Zheng, D. J. Yang, H.W. Liu and H. Y. Zhu, *J. Hazard. Mater*. 2013, 246-247, 199-205.

20. S. S. Liu, N. Wang, Y.C. Zhang, Y.R. Li, Z. Han and P. Na, *J. Hazard. Mater*. 2015,284, 171-181.

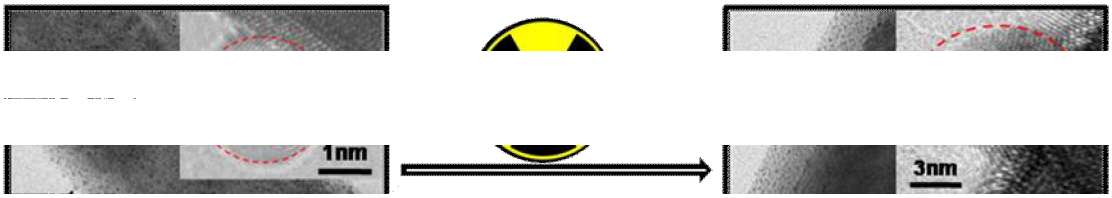

To capture radioactive iodine from wastewater, the Ag_2O particles anchored firmly onto the $Nb_2Na_2O_6 \cdot H_2O$ nanofibers with a large specific surface area that allows them to disperse sufficiently without forming aggregates.